Research Article

Study of Proton, Deuteron, and Triton at 54.4 GeV

M. Waqas[1] and G. X. Peng (ID)[1,2,3]

[1]*School of Nuclear Science and Technology, University of Chinese Academy of Sciences, Beijing 100049, China*
[2]*Theoretical Physics Center for Science Facilities, Institute of High Energy Physics, Beijing 100049, China*
[3]*Synergetic Innovation Center for Quantum Effects & Application, Hunan Normal University, Changsha 410081, China*

Correspondence should be addressed to G. X. Peng; gxpeng@ucas.ac.cn

Transverse momentum spectra of proton, deuteron, and triton in gold-gold (Au-Au) collisions at 54.4 GeV are analyzed in different centrality bins by the blast wave model with Tsallis statistics. The model results are approximately in agreement with the experimental data measured by STAR Collaboration in special transverse momentum ranges. We extracted the kinetic freeze-out temperature, transverse flow velocity, and freeze-out volume from the transverse momentum spectra of the particles. It is observed that the kinetic freeze-out temperature is increasing from the central to peripheral collisions. However, the transverse flow velocity and freeze-out volume decrease from the central to peripheral collisions. The present work reveals the mass dependent kinetic freeze-out scenario and volume differential freeze-out scenario in collisions at STAR Collaboration. In addition, parameter q characterizes the degree of nonequilibrium of the produced system, and it increases from the central to peripheral collisions and increases with mass .

1. Introduction

The two important stages in the evolution system are chemical and kinetic freeze-out. The degree of excitation of the interacting system at the two stages is different from each other. The chemical and kinetic freeze-out temperatures are used to describe different excitation degrees of interacting system of the two stages. In general, the ratios of different kinds of particles are no longer changed at the stage of chemical freeze-out. The chemical freeze-out temperature can be obtained from different particle ratios in the framework of the thermal model [1–3]. The transverse momentum spectra of different particles are no longer changed at the stage of kinetic freeze-out and thermal/kinetic freeze-out temperature can be obtained from the transverse momentum spectra according to the hydrodynamical model [4].

It is important to point out that the transverse momentum spectra even though in a narrow p_T range, but it contains both the contribution of thermal motion and transverse flow velocity. The random thermal motion reflects the excitation,

and the transverse flow velocity reflects the degree of expansion of the interacting system. In order to extract the kinetic freeze-out temperature (T_0), we have excluded the contribution of transverse flow velocity (β_T), that is, to disengage the random thermal motion and transverse flow velocity. There are various methods to disengage the two issues. The methods include but are not limited to blast wave fit with Boltzmann Gibbs statistics [5–7], blast wave model with Tsallis statistics [8–10], and alternative methods [11–17].

The dependence of T_0 and β_T on centrality is a very complex situation. There are two schools of thought. (1) T_0 increase decrease from the central to peripheral collisions [18–21] and (2) T_0 increase from the central to peripheral collisions [22, 23]. Both have their own explanations. Larger T_0 in the central collisions explain higher degree of excitation of the system due to more violent collisions, while smaller T_0 in the central collisions indicates longer lived fireball in the central collisions. It is very important to find out which collision system contains larger T_0. Furthermore, there are several opinions about the freeze-out of particles which
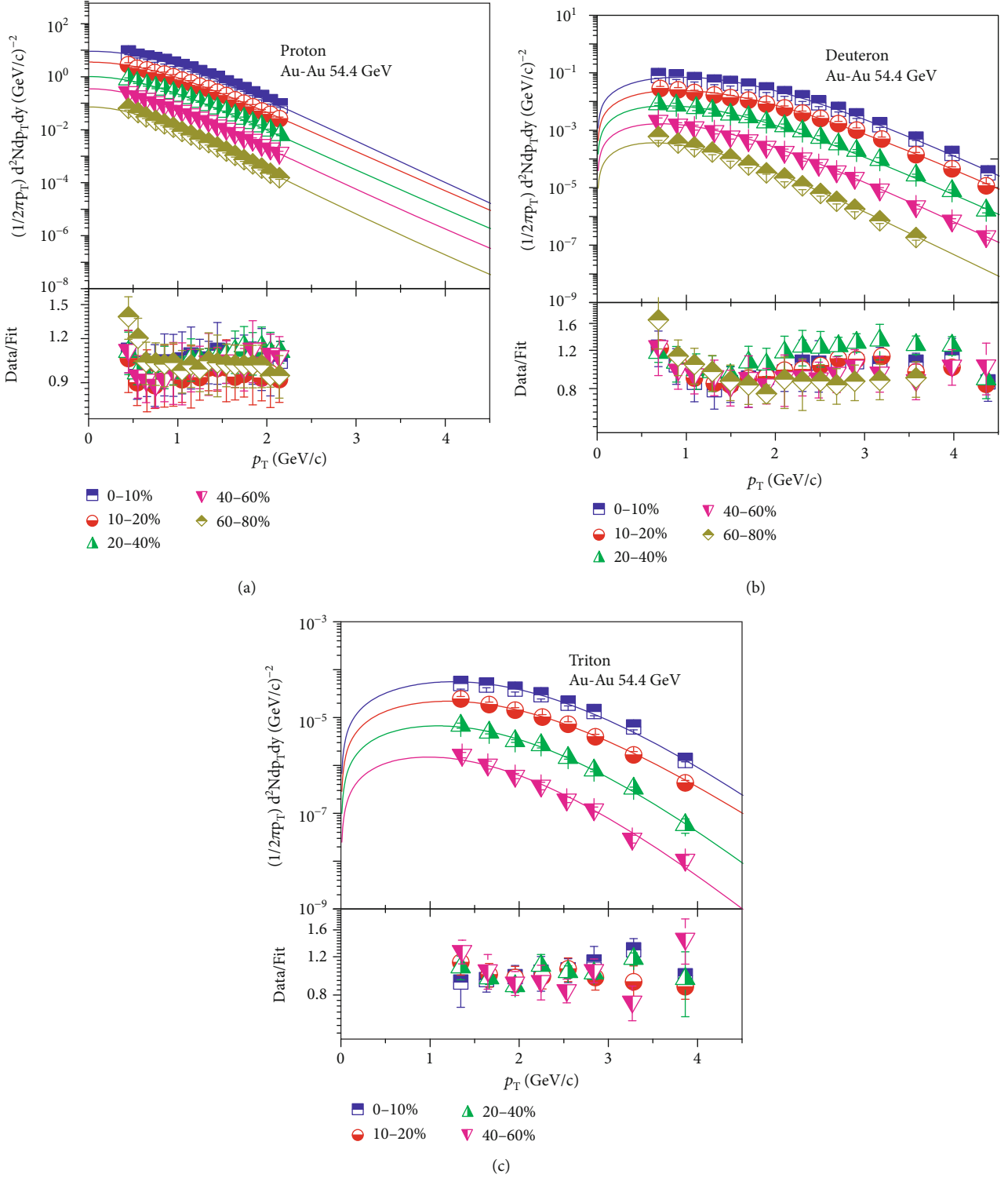
(a)

(b)

(c)

FIGURE 1: Transverse mass spectra of (a–c) p, d, and t produced in different centrality bins in Au-Au collisions at $\sqrt{sNN} = 54.4$ GeV. The symbols represent the experimental data measured by the STAR Collaboration at $|y| < 0.5$ [40]. The curves are our fitted results by Equation (1). Each panel is followed by its corresponding ratios of data/fit.

include single, double, and multiple kinetic freeze-out. It is also very important to dig out the correct freeze-out scenario.

In the present work, we will analyze the p_T spectra of proton, deuteron, and triton and will extract T_0 and β_T. Deu-

teron and triton are light nuclei. The fundamental mechanism for light nuclei production in relativistic heavy ion collision is not well understood [24–26]. Coalescence of anti(nucleons) is a possible approach [27–31]. Because of

TABLE 1: Values of free parameters (T_0 and β_T), entropy index (q), normalization constant (N_0), χ^2, and degree of freedom (dof) corresponding to the curves in Figures 1.

Collisions	Centrality	Particle	T_0	β_T	V (fm^3)	q	N_0	χ^2/dof
	0–10%	p	0.082 ± 0.006	0.454 ± 0.009	4000 ± 220	1.012 ± 0.004	0.019 ± 0.005	5/13
	10–20%	—	0.086 ± 0.005	0.434 ± 0.008	3800 ± 300	1.015 ± 0.005	0.0072 ± 0.0004	6/13
	20–40%	—	0.090 ± 0.007	0.420 ± 0.010	3650 ± 234	1.018 ± 0.007	0.00194 ± 0.0005	11/13
	40–60%	—	0.094 ± 0.006	0.370 ± 0.008	3400 ± 190	1.022 ± 0.006	$6 \times 10^{-4} \pm 6 \times 10^{-5}$	7/13
	60–80%	—	0.099 ± 0.002	0.340 ± 0.011	3100 ± 200	1.024 ± 0.007	$1.2 \times 10^{-4} \pm 4 \times 10^{-5}$	29/13
	0–10%	d	0.127 ± 0.007	0.360 ± 0.010	3000 ± 177	1.004 ± 0.006	$4.15 \times 10^{-4} \pm 4 \times 10^{-5}$	10/12
Figure 1	10–20%	—	0.130 ± 0.005	0.340 ± 0.009	2700 ± 220	1.007 ± 0.005	$1.5 \times 10^{-5} \pm 5 \times 10^{-5}$	11/12
Au-Au 54.4 GeV	20–40%	—	0.134 ± 0.005	0.280 ± 0.010	2500 ± 180	1.011 ± 0.004	$5.1 \times 10^{-5} \pm 6 \times 10^{-6}$	39/12
	40–60%	—	0.138 ± 0.006	0.224 ± 0.008	2200 ± 200	1.013 ± 0.005	$1.2 \times 10^{-6} \pm 6 \times 10^{-6}$	3/12
	60–80%	—	0.142 ± 0.008	0.130 ± 0.009	2000 ± 200	1.016 ± 0.006	$2.7 \times 10^{-7} \pm 4 \times 10^{-7}$	16/10
	0–10%	t	0.136 ± 0.005	0.340 ± 0.007	2200 ± 165	1.0002 ± 0.004	$9.17 \times 10^{-7} \pm 3 \times 10^{-8}$	4/3
	10–20%	—	0.139 ± 0.006	0.320 ± 0.009	2000 ± 150	1.0006 ± 0.006	$4 \times 10^{-7} \pm 4 \times 10^{-8}$	3/3
	20–40%	—	0.148 ± 0.007	0.250 ± 0.008	1823 ± 135	1.0009 ± 0.007	$1.4 \times 10^{-8} \pm 6 \times 10^{-8}$	12/8
	40–60%	—	0.154 ± 0.006	0.170 ± 0.010	1500 ± 180	1.0012 ± 0.006	$3.7 \times 10^{-6} \times 10^{-9}$	6/3

small binding energies (d with 2.2 MeV and t with 8.8 MeV), the light nuclei cannot persists when the temperature is much higher than their binding energy. The typical kinetic freeze-out temperature is around 100 MeV for light hadrons, so they might disintegrate and be formed again by final-state coalescence after nucleons are decoupled from the hot and dense system. Hence, the study of the light nuclei can be useful in the extraction of information of nucleon distribution at the freeze-out [27, 30, 32].

Before going to the formalism, we would point out that the concept of the volume is also important in high-energy collisions. The volume occupied by the ejectiles, when the mutual interactions become negligible and the only force they feel is the columbic repulsive force, is called the kinetic freeze-out volume (V). Various freeze-out volumes occur at various freeze-out stages, but we are only focusing on the kinetic freeze-out volume V in the present work. The freeze-out volume gives information about the coexistence of phase transition and is important in the extraction of multiplicity, microcanonical heat capacity, and its negative branch or shape of the caloric curves under the thermal constraints can be obtained V.

The remainder of the paper consists of method and formalism in Section 2, followed by the results and discussion in Section 3. In Section 4, we summarized our main observations and conclusions.

2. The Method and Formalism

In high-energy collisions, there are two types of particle production process: (1) soft process ad (2) hard process. For soft process, there are various methods which include but are not limited to blast wave model with boltzmann Gibbs statistics [5–7], blast wave model with Tsallis statistics [8–10], Hage-

dorn thermal model [20], and standard distribution [33, 34]. We are interested in the blast wave model with Tsallis statistics. According to [8], the blast wave fit with Tsallis statistics results in the probability density function be

$$
f_1(p_T) = \frac{1}{N}\frac{dN}{dp_T} = C\frac{gV}{(2\pi)^2}p_T m_T \int_{-\pi}^{\pi} d\phi \int_0^R r\,dr
$$
$$
\times \left\{ 1 + \frac{q-1}{T_0}\left[m_T \cosh(\rho) - p_T \sinh(\rho) \times \cos(\phi)\right] \right\}^{-1/(q-1)},
$$

(1)

where C denotes the normalization constant that leads the integral in Equation (1) to be normalized to 1, g is the degeneracy factor which is different for different particles based on $g_n = 2S_n + 1$, $m_T = \sqrt{p_T^2 + m_0^2}$ is the transverse mass, m_0 denotes rest mass of the particle, ϕ shows the azimuthal angle, r is the radial coordinate, R is the maximum r, q represents the measure of degree of deviation of the system from an equilibrium state, $\rho = \tanh^{-1}[\beta(r)]$ is the boost angle, $\beta(r) = \beta S(r/R)^{n0}$ is a self-similar flow profile, β_S represents the flow velocity on the surface, as a mean of $\beta(r)$, $\beta(r) = (2/R^2)\int_0^R r\beta(r)dr = 2\beta_s/(n_0 + 2) = 2\beta_s/3$, and $n_0 = 1$. Furthermore, the index $-1/(q-1)$ in Equation (1) can be substituted by $-q/(q-1)$ due to the reason that q is being close to 1. This substitution results in a small and negligible divergence in the Tsallis distribution.

In case of a not too wide p_T range, the above equation can be used to describe the p_T spectra and we can extract T_0 and β_T. But, if we use the wide p_T spectra, then the contribution of the hard scattering process can be considered. According to quantum chromodynamics (QCD) calculus [35–37], the contribution of hard process is parameterized to be an
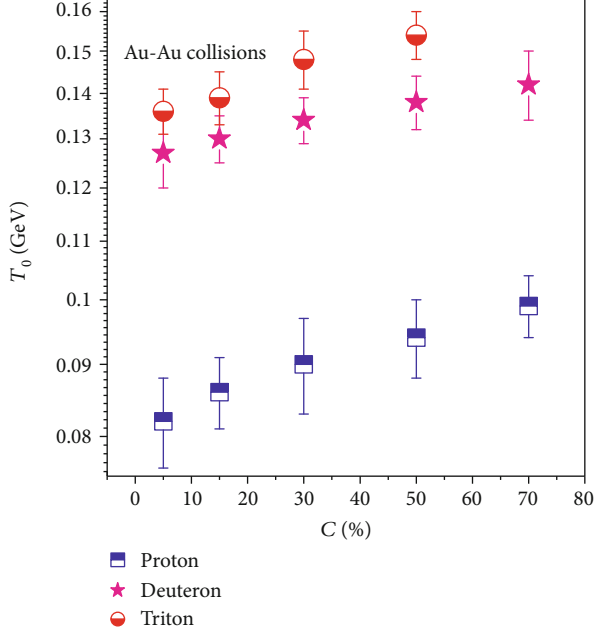
Figure 2: The dependence of T_0 on centrality.

Figure 3: The dependence of β_T on centrality.

inverse power law.

$$f_H(p_T) = \frac{1}{N}\frac{dN}{dp_T} = Ap_T\left(1 + \frac{p_T}{p_0}\right)^{-n}, \qquad (2)$$

which is the Hagedorn function [38, 39], A is the normalization constant while p_0 and n are the free parameters.

The superposition of the soft and hard scattering processes can be used if the p_T spectra are distributed in a wide range. If Equation (1) describes the contribution of the soft process, then the contribution of the hard process can be described by Equation (2). To describe the spectrum in a wide p_T range, one can superpose the two-component superposition like this
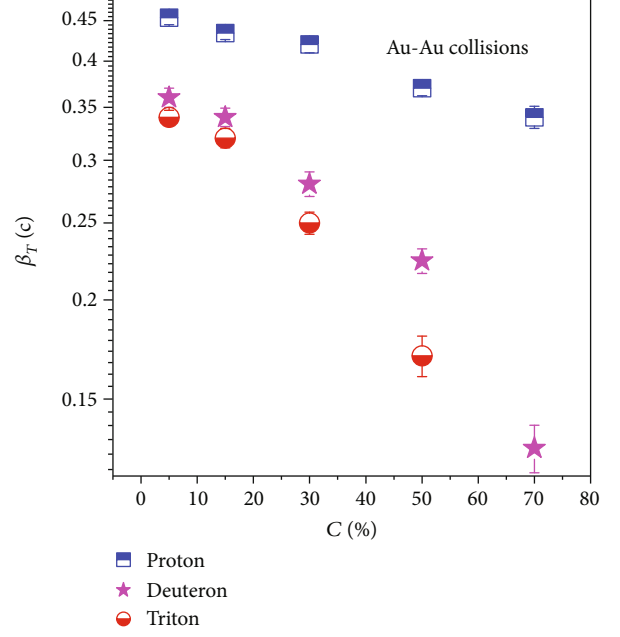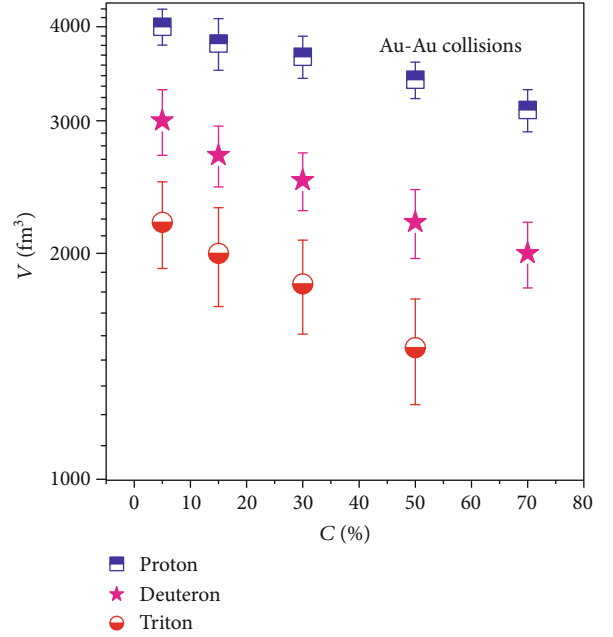
$$f_0(p_T) = kf_S(p_T) + (1 - k)f_H(p_T), \qquad (3)$$

where k denotes the contribution fraction of soft excitation and $(1 - k)$ shows the hard scattering process, f_S denotes the soft process which contributes in the low p_T region and f_H is the hard process which contributes in a whole p_T region. The two contributions overlap each other in the low p_T region.

We may also use the usual step function to superpose the two functions. According to the Hagedorn model [38],

$$f_0 = (p_T) = A_1\theta(p_1 - p_T)f_S(p_T) + A_2\theta(p_T - p_1)f_H(p_T), \qquad (4)$$

where A_1 and A_2 are the normalization constants that synthesize $A_1f_S(p_1) = A_1f_H(p_1)$ and $\theta(x)$ is the usual step function.

Figure 4: The dependence of V on centrality.

3. Results and Discussion

Figure 1 presents the transverse momentum (p_T) spectra [$($ $1/2\pi p_T) \, d^2N/dydp_T$] of proton, deuteron, and triton in Au-Au collisions at $\sqrt{sNN} = 54.4\,\text{GeV}$. The p_T spectra is distributed in different centrality bins of 0–10%, 10–20%, 20–40%, 40–60%, and 60–80% for p and d, and 0–10%, 10–20%, 20–40%, and 40–60% for triton at $|y| < 0.5$, where $|y|$ denotes the rapidity. The symbols represent the experimental data measured by the STAR Collaborations [40], and the curves
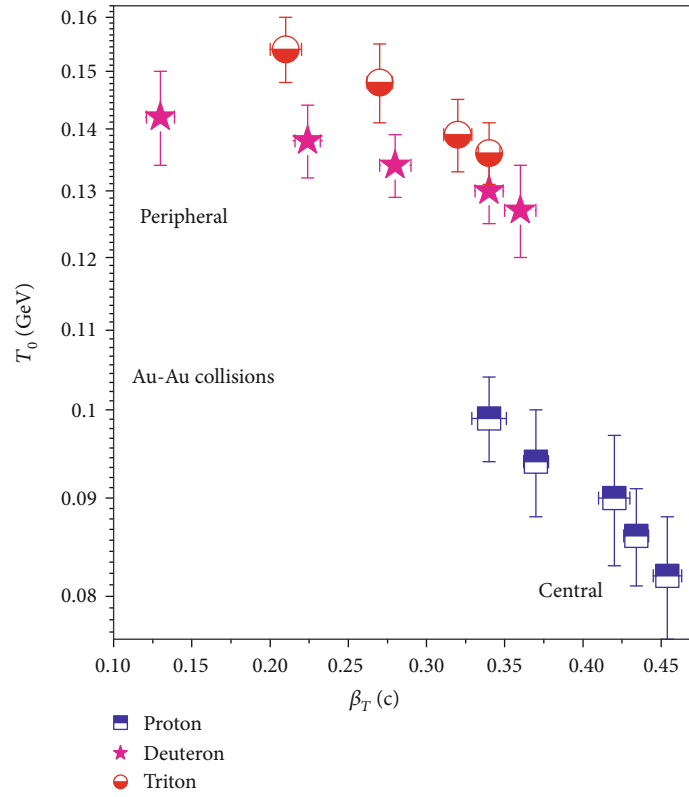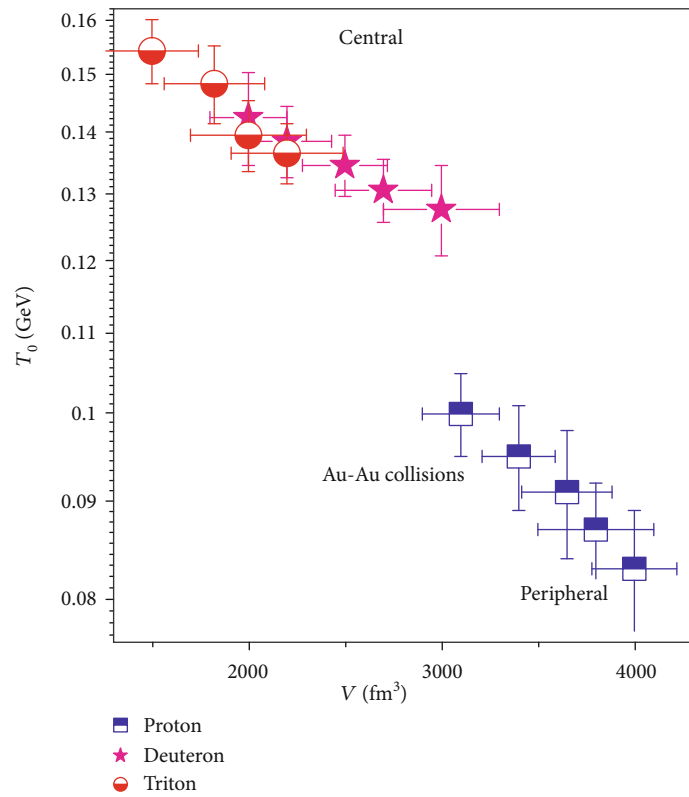
FIGURE 5: Variation of T_0 with β_T.

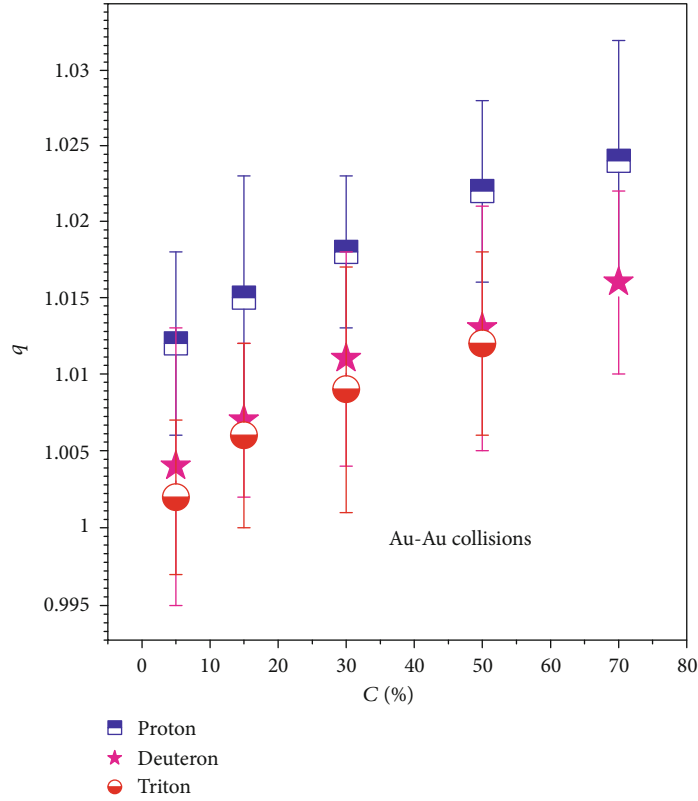FIGURE 6: Variation of T_0 with V.

FIGURE 7: Dependence of q on centrality.

are our fitting results by using the blast wave model with Tsallis statistics. Each panel is followed by its corresponding data/fit. The related parameters, χ^2 and degree of freedom (dof) are listed in Table 1. One can see that Equation (1) fits well the data in Au-Au collisions at 54.4 GeV at the RHIC.

To show the trend of the extracted parameters, Figure 2 shows the dependence of kinetic freeze-out temperature on centrality. One can see that T_0 in central collisions is smaller, and it is increasing with the decrease of centrality which indicates a decrease of lifetime of fireball from central collisions to peripheral collisions. Furthermore, T_0 is observed to be mass dependent, as it is larger from triton, followed by deuteron and then proton which means heavy particles freeze-out early than lighter particles.

Figure 3 shows the centrality dependence of transverse flow velocity. β_T is observed to decrease with the decrease of centrality due to the reason that in central collisions the system undergoes more violent collisions and the system expands very rapidly. In addition, β_T is observed for smaller for heavy particles.

Figure 4 is same as Figure 3 but shows the centrality-dependent freeze-out volume. The freeze-out volume decreases with the decrease of centrality due to decreasing the number of participant nucleons. There are large number of binary collisions due to the rescattering of partons in central collisions, and therefore, the system with more participants reaches quickly to the equilibrium state. Furthermore, the volume differential scenario is observed and heavy particles are observed to have less freeze-out volume and this

shows the early freeze-out heavier particles. The different freeze-out of different particles exhibits different freeze-out surfaces of different particles. Figures 5 and 6 are the same. Figure 5 shows the correlation of T_0 and β_T and Figure 6 shows the correlation of T_0 and V. One can see that both T_0 and β_T, and T_0 and V exhibit a two-dimensional anticorrelation band. The larger the T_0, the smaller the β and V. Figure 7 shows the dependence of q on centrality. The parameter q is smaller in central collisions, but as we go from the central to peripheral collisions, it is going to increase. The parameter is varying with mass of the particle, larger q is observed for light particles. The interacting system stays at equilibrium because q is being very close to 1. In Figure 8, the parameter N_0 decreases with the mass of the particle. N_0 basically shows the multiplicity, and it is larger in the central collision which decreases towards periphery.

3.1. Further Discussion. The study of p_T spectra of the particles may give some fruitful information about effective temperature (T_{eff}), initial temperature (T_i), thermal/kinetic freeze-out temperature (T_0), thermal freeze-out volume (V) of the interacting system, and transverse flow velocity (β_T) of the final-state particles. We use the fitting method to extract this information by using different models and distributions. In the present work, the blast wave model with Tsallis statistics is used.

The structure of transverse momentum (p_T) spectra of charged particles generated in high-energy heavy ion collisions is very complex. It is not enough to use only one
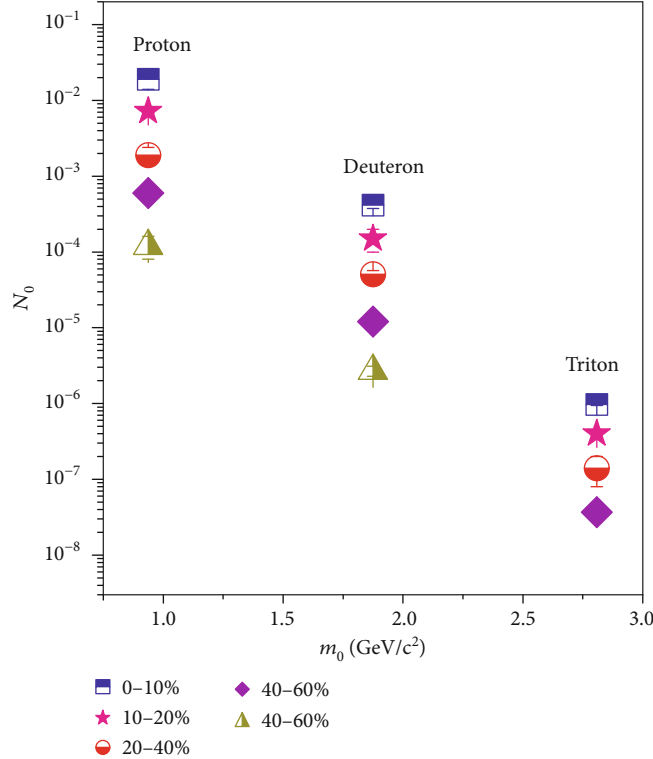
FIGURE 8: Dependence of N_0 on mass and centrality.

probability density function to describe the p_T spectra, though this function can be of various forms, particularly, in the case when the maximum p_T reaches to 100 GeV at LHC collisions [41]. Several p_T regions are observed by the model analysis [42], including the first region $p_T < 4$ -6 GeV/c, $4 - 6$ GeV/c $< p_T < 17 - 20$ GeV/c, and the third region with $p_T > 17 - 20$ GeV/c. The boundaries of different p_T regions at the RHIC are slightly lower. It is expected that different p_T regions correspond to different interacting mechanisms. Even for the same p_T region, there are different explanations due to different model methods and microcosmic pictures.

According to [42], different whole features of fragmentation and hadronization of partons through the string dynamics corresponds to different p_T regions. The effects and changes by the medium take part in the main role in the first p_T region, while it has weak appearance in second p_T region. At the same time, in the third region, the nuclear transparency results in a negligible impact of the medium. From number of strings' point of view, the maximum number of strings is in the second p_T region that results in fusion and creation of strings and collective behavior of partons. The second p_T region is proposed as a possible area of quark-gluon plasma (QGP) through the string fusion. Due to direct hadronization of the low-energy strings into mesons [42], the first p_T region has the minimum number of strings and maximum number of hadrons. In some cases, there may be the contribution region ($p_T < 0.2$-0.3 GeV/c) of the very soft process which is due to resonant production of charged particles, e.g., pions, and this region is considered as the fourth p_T

region. Different components in a unified superposition can describe the four p_T regions. We have two methods in order to structure the unified superposition. The first method is the common method of overlapping of the contribution regions of various components; however, the second method is the Hagedorn model [38] which excludes this overlapping. If the contribution of the hard component in the first method is neglected in the low p_T region due to its small value, the first method can be changed into the second method. Indeed the contribution to T_0 and β_T is less for the hard component. If the spectra in the low p_T region is analyzed to extract only T_0 and β_T, then we can give up the second part of Equations (3) and (4). That is, $f_S(p_T)$ can be used directly from Equation (1) which also includes the contribution of the very soft component that comes from resonance decays if available in the data. In the present work, the contribution of the hard component in the low p_T region if available is included in the extraction of T_0 and β_T which may cause a slight increase in T_0 and/or β_T but the relative increase can be neglected due to small values [43]. In the present work, we only use Equation (1), which means that the fraction of the hard component is zero in the low p_T region. But, we also show Equations (3) and (4) to show a method for further analysis if necessary.

4. Conclusions

The main observations and conclusions are summarized here.

(a) The transverse momentum spectra of proton (p), deuteron (d), and triton (t) are analyzed by the blast wave model with Tsallis statistics and the bulk properties in terms of the kinetic freeze-out temperature, transverse flow velocity, and kinetic freeze-out volume are extracted

(b) The kinetic freeze out temperature (T_0) is observed to increase from the central to peripheral collisions. However, the transverse flow velocity and freeze-out volume is decreasing from the central to peripheral collisions

(c) The entropy index (q) increasing with from centrality while parameter N_0 is decreasing with centrality

(d) The kinetic freeze-out temperature, transverse flow velocity, and freeze-out volume decrease with the increasing mass of the particle. Therefore, the mass differential kinetic freeze-out scenario and volume differential freeze out scenario are observed

(e) Both the entropy index (q) and the parameter N_0 decrease with the mass of particle

Data Availability

The data used to support the findings of this study are included within the article and are cited at relevant places within the article with in the text as references.

Ethical Approval

The authors declare that they are in compliance with ethical standards regarding the content of this paper.

Disclosure

The funding agencies have no role in the design of this study; in the collection, analysis, or interpretation of the data in writing the manuscript; or in the decision to publish the results.

Conflicts of Interest

The authors declare that there are no conflicts of interest regarding the publication of this paper.

References

[1] J. Cleymans, H. Oeschler, K. Redlich, and S. Wheaton, "Comparison of chemical freeze-out criteria in heavy-ion collisions," *Physical Review C*, vol. 73, no. 3, article 034905, 2006.

[2] A. Andronic, P. Braun-Munzinger, and J. Stachel, "The horn, the hadron mass spectrum and the QCD phase diagram – the statistical model of hadron production in central nucleus-nucleus collisions," *Nuclear Physics A*, vol. 834, no. 1-4, pp. 237c–240c, 2010.

[3] A. Andronic, P. Braun-Munzinger, and J. Stachel, "Thermal hadron production in relativistic nuclear collisions," *Acta Physica Polonica B*, vol. 40, pp. 1005–1012, 2009.

[4] Y. Hama and F. S. Navarra, "Energy and mass-number dependence of the dissociation temperature in hydrodynamical models," *Zeitschrift für Physik C Particles and Fields*, vol. 53, no. 3, pp. 501–506, 1992.

[5] E. Schnedermann, J. Sollfrank, and U. Heinz, "Thermal phenomenology of hadrons from 200AGeV S+S collisions," *Physical Review C*, vol. 48, no. 5, pp. 2462–2475, 1993.

[6] STAR Collaboration, "Systematic measurements of identified particle spectra in pp, $d+Au$, and $Au+Au$ collisions at the STAR detector," *Physical Review C*, vol. 79, no. 3, article 034909, 2009.

[7] STAR Collaboration, "Identified particle production, azimuthal anisotropy, and interferometry measurements in $Au+Au$ collisions at $\sqrt{s_{NN}} = 9.2GeV$," *Physical Review C*, vol. 81, no. 2, article 024911, 2010.

[8] Z. Tang, Y. Xu, L. Ruan, G. van Buren, F. Wang, and Z. Xu, "Spectra and radial flow in relativistic heavy ion collisions with Tsallis statistics in a blast-wave description," *Physical Review C*, vol. 79, no. 5, article 051901, 2009.

[9] Z.-B. Tang, L. Yi, L.-J. Ruan et al., "The statistical origin of constituent-quark scaling in QGP hadronization," *Chinese Physics Letters*, vol. 30, no. 3, article 031201, 2013.

[10] K. Jiang, Y. Zhu, W. Liu et al., "Onset of radial flow in $p+p$ collisions," *Physical Review C*, vol. 91, no. 2, article 024910, 2015.

[11] S. Takeuchi, K. Murase, T. Hirano, P. Huovinen, and Y. Nara, "Effects of hadronic rescattering on multistrange hadrons in high-energy nuclear collisions," *Physical Review C*, vol. 92, no. 4, article 044907, 2015.

[12] H. Heiselberg and A. M. Levy, "Elliptic flow and Hanbury-Brown–Twiss correlations in noncentral nuclear collisions," *Physical Review C*, vol. 59, no. 5, pp. 2716–2727, 1999.

[13] U. W. Heinz, *Concepts of heavy-ion physics. Lecture notes for lectures presented at the 2nd CERNC Latin-American school of high-energy physics*, San Miguel Regla, Mexico, 2003 http://arxiv.org/abs/hepph/0407360.

[14] R. Russo, *Measurement of D^+ meson production in p-Pb collisions with the ALICE detector*, PhD Thesis, Universita degli Studi di Torino, Italy, 2015, http://arxiv.org/abs/1511.04380.

[15] H.-R. Wei, F. H. Liu, and R. A. Lacey, "Kinetic freeze-out temperature and flow velocity extracted from transverse momentum spectra of final-state light flavor particles produced in collisions at RHIC and LHC," *The European Physical Journal A*, vol. 52, no. 4, p. 102, 2016.

[16] H.-L. Lao, H.-R. Wei, F.-H. Liu, and R. A. Lacey, "An evidence of mass-dependent differential kinetic freeze-out scenario observed in Pb-Pb collisions at 2.76 TeV," *The European Physical Journal A*, vol. 52, no. 7, p. 203, 2016.

[17] H. R. Wei, F.-H. Liu, and R. A. Lacey, "Disentangling random thermal motion of particles and collective expansion of source from transverse momentum spectra in high energy collisions," *Journal of Physics G: Nuclear and Particle Physics*, vol. 43, no. 12, article 125102, 2016.

[18] M. Waqas, F.-H. Liu, S. Fakhraddin, and M. A. Rahim, "Possible scenarios for single, double, or multiple kinetic freeze-out in high-energy collisions," *Indian Journal of Physics*, vol. 93, no. 10, pp. 1329–1343, 2019.

[19] M. Waqas and F.-H. Liu, "Centrality dependence of kinetic freeze-out temperature and transverse flow velocity in high energy nuclear collisions," 2018, http://arxiv.org/abs/1806.05863.

[20] M. Waqas and F.-H. Liu, "Initial, effective, and kinetic freeze-out temperatures from transverse momentum spectra in high-energy proton(deuteron)–nucleus and nucleus–nucleus collisions," *The European Physical Journal Plus*, vol. 135, no. 2, p. 147, 2020.

[21] Q. Wang and F.-H. Liu, "Initial and final state temperatures of antiproton emission sources in high energy collisions," *International Journal of Theoretical Physics*, vol. 58, no. 12, pp. 4119–4138, 2019.

[22] L. Kumar and STAR Collaboration, "Systematics of kinetic freeze-out properties in high energy collisions from STAR," *Nuclear Physics A*, vol. 931, pp. 1114–1119, 2014.

[23] STAR Collaboration, "Bulk properties of the medium produced in relativistic heavy-ion collisions from the beam energy scan program," *Physical Review C*, vol. 96, no. 4, article 044904, 2017.

[24] STAR Collaboration, "Measurement of elliptic flow of light nuclei at $\sqrt{s_{NN}}$ = 200, 62.4, 39, 27, 19.6, 11.5, and 7.7 GeV at the BNL relativistic heavy ion collider," *Physical Review C*, vol. 94, article 034908, 2016.

[25] ALICE Collaboration, "Production of light nuclei and antinuclei inppand Pb-Pb collisions at energies available at the CERN Large Hadron Collider," *Physical Review C*, vol. 93, no. 2, article 024917, 2016.

[26] J. Chen, D. Keane, Y. G. Ma, A. Tang, and Z. Xu, "Antinuclei in heavy-ion collisions," *Physics Reports*, vol. 760, pp. 1–39, 2018.

[27] H. H. Gutbrod, A. Sandoval, P. J. Johansen et al., "Final-state interactions in the production of hydrogen and helium isotopes by relativistic heavy ions on uranium," *Physical Review Letters*, vol. 37, no. 11, pp. 667–670, 1976.

[28] R. Scheibl and U. Heinz, "Coalescence and flow in ultrarelativistic heavy ion collisions," *Physical Review C*, vol. 59, no. 3, pp. 1585–1602, 1999.

[29] W. J. Llope, S. E. Pratt, N. Frazier et al., "The fragment coalescence model," *Physical Review C*, vol. 52, no. 4, pp. 2004–2012, 1995.

[30] H. Sato and K. Yazaki, "On the coalescence model for high energy nuclear reactions," *Physics Letters B*, vol. 98, no. 3, pp. 153–157, 1981.

[31] K.-J. Sun, L.-W. Chen, C. M. Ko, and Z. Xu, "Probing QCD critical fluctuations from light nuclei production in relativistic heavy-ion collisions," *Physics Letters B*, vol. 774, pp. 103–107, 2017.

[32] S. T. Butler and C. A. Pearson, "Deuterons from high-energy proton bombardment of matter," *Physical Review*, vol. 129, no. 2, pp. 836–842, 1963.

[33] M. Waqas, F. H. Liu, and Z. Wazir, "Dependence of temperatures and kinetic freeze-out volume on centrality in Au-Au and Pb-Pb collisions at high energy," *Advances in High Energy Physics*, vol. 2020, Article ID 8198126, 15 pages, 2020.

[34] M. Waqas, F.-H. Liu, L. L. Li, and H. M. Alfanda, "Effective (kinetic freeze-out) temperature, transverse flow velocity, and kinetic freeze-out volume in high energy collisions," *Nuclear Science and Techniques*, vol. 31, no. 11, p. 109, 2020.

[35] R. Odorico, "Does a transverse energy trigger actually trigger on large-PT jets?," *Physics Letters B*, vol. 118, no. 1-3, pp. 151–154, 1982.

[36] UA1 Collaboration, "Transverse momentum spectra for charged particles at the CERN proton-antiproton collider," *Physics Letters B,* vol. 118, no. 1-3, pp. 167–172, 1982.

[37] T. Mizoguchi, M. Biyajima, and N. Suzuki, "Analyses of whole transverse momentum distributions in $p\bar{p}$ and pp collisions by using a modified version of Hagedorn's formula," *International Journal of Modern Physics A*, vol. 32, no. 11, article 1750057, 2017.

[38] R. Hagedorn, "Multiplicities,p T distributions and the expected hadron → quark-gluon phase transition," *La Rivista del Nuovo Cimento*, vol. 6, no. 10, pp. 1–50, 1983.

[39] ALICE Collaboration, "Production of $\Sigma(1385)^{\pm}$ and $\Xi(1530)^{0}$ in proton–proton collisions at $\sqrt{s}$ = 7 TeV," *The European Physical Journal C*, vol. 75, no. 1, p. 1, 2015.

[40] D. Zhang and STAR Collaboration, "Light Nuclei (*d, t*) Production in Au + Au Collisions at $\sqrt{s_{NN}}$ = 7.7 − 200 GeV," *Nuclear Physics A*, vol. 1005, article 121825, 2021.

[41] CMS Collaboration, "Study of high-p T charged particle suppression in PbPb compared to pp collisions at $\sqrt{s_{NN}}$ = 2.76 TeV," *The European Physical Journal C*, vol. 72, no. 3, article 1945, 2012.

[42] M. K. Suleymanov, "The meaning behind observed pT regions at the LHC energies," *International Journal of Modern Physics E*, vol. 27, no. 1, article 1850008, 2018.

[43] H.-L. Lao, F.-H. Liu, B.-C. Li, M.-Y. Duan, and R. A. Lacey, "Examining the model dependence of the determination of kinetic freeze-out temperature and transverse flow velocity in small collision system," *Nuclear Science and Techniques*, vol. 29, no. 11, p. 164, 2018.